JOURNAL OF GUIDANCE, CONTROL, AND DYNAMICS
Vol. 17, No. 2, March–April 1994

Homotopy Algorithm for Maximum Entropy Design

Emmanuel G. Collins Jr.,* Lawrence D. Davis,* and Stephen Richter†
Harris Corporation, Melbourne, Florida 32902

Maximum entropy design is a generalization of the LQG method that was developed to enable the synthesis of robust control laws for flexible structures. The method was developed by Hyland and motivated by insights gained from statistical energy analysis. Maximum entropy design has been used successfully in control design for ground-based structural testbeds and certain benchmark problems. The maximum entropy design equations consist of two Riccati equations coupled to two Lyapunov equations. When the uncertainty is zero, the equations decouple and the Riccati equations become the standard LQG regulator and estimator equations. A previous homotopy algorithm to solve the coupled equations relies on an iterative scheme that exhibits slow convergence properties as the uncertainty level is increased. This paper develops a new homotopy algorithm that does not suffer from this defect and in fact can have quadratic convergence rates along the homotopy curve. Algorithms of this type should also prove effective in the solution of other sets of coupled Riccati and Lyapunov equations appearing in robust control theory.

Nomenclature

$e_m^{(i)}$ = m-dimensional column vector whose ith element equals one and whose additional elements are zeros
I_r = $r \times r$ identity matrix
$\mathbb{R}^n$, $\mathbb{R}^{m \times n}$ = $n \times 1$ real vectors, $m \times n$ real matrices
tr Z = trace of square matrix Z
vec$(\cdot)$ = invertible linear operator defined such that $\mathrm{vec}(S) \triangleq [s_1^T s_2^T \cdots s_q^T]^T$, $S \in \mathbb{R}^{p \times q}$ where $s_j \in \mathbb{R}^p$ denotes the jth column of S
$Y > Z$ = $Y - Z$ is positive definite
$Y \geq Z$ = $Y - Z$ is nonnegative definite
Y/Z = matrix whose (i,j) element is y_{ij}/z_{ij}, Y and Z must have identical dimensions (MATLAB notation)
$Y * Z$ = Hadamard product of Y and Z $([y_{ij} z_{ij}])$, Y and Z must have identical dimensions
Z^* = complex conjugate of the matrix Z
Z^H = complex conjugate transpose of the matrix Z, $(Z^*)^T$
$Z(k,:)$ = kth row of the matrix Z (MATLAB notation)
$Z(:,k)$ = kth column of the matrix Z (MATLAB notation)
z_{ij}, $Z_{i,j}$, or $Z_{(i,j)}$ = (i,j) element of matrix Z
$\otimes$ = Kronecker product[14]

I. Introduction

THE linear-quadratic-Gaussian (LQG) compensator[1] has been developed to facilitate the design of control laws for complex, multi-input/multi-output (MIMO) systems such as flexible structures. However, it is well known that an LQG compensator can yield a closed-loop system with arbitrarily poor robustness properties.[2] This deficiency has led to generalizations of LQG that allow the design of robust controllers. One such generalization of LQG is the maximum entropy control design approach that was originated by Hyland[3] and Bernstein and Hyland.[4,5] Maximum entropy control design was developed specifically to enable robust control law design for flexible structures. In particular, this design technique develops control laws that are insensitive to changes in the (undamped) modal frequencies. The approach was motivated by insights from statistical energy analysis and has proven to be an effective tool in the design of robust control laws for ground-based flexible structure testbeds[6,7] and for certain benchmark problems.[8-10]

The rigorous theoretical foundation for maximum entropy design is not yet complete. However, in Ref. 11 it is shown that, for an open-loop system, a Lyapunov function based on the maximum entropy constraint equation predicts unconditional stability for changes in the undamped natural frequency. The results of Ref. 11 also provide evidence that the theoretical foundation of maximum entropy analysis and design may be related to recent robustness results based on parameter-dependent Lyapunov functions.[12]

The computation of full-order maximum entropy controllers requires the solution of a set of equations consisting of two Riccati equations coupled to two Lyapunov equations. If the uncertainty is assumed to be zero, these equations decouple and the Riccati equations become the standard LQG Riccati equations. A homotopy algorithm for solving these equations is described in Ref. 13. This algorithm is based on first solving an LQG problem and gradually increasing the uncertainty level until the desired degree of robustness is achieved. Unfortunately, the algorithm of Ref. 13 relies on an iterative scheme that tends to have increasingly poor convergence properties as the uncertainty level is increased.

The contribution of this paper is the development of a new homotopy algorithm for full-order maximum entropy design. Unlike the previous approach, this algorithm can have quadratic convergence rates along the homotopy curve. Algorithms of this type should also prove effective in the solution of other sets of coupled Riccati and Lyapunov equations appearing in robust control theory (e.g., Ref. 12). The algorithm has been implemented in MATLAB and is illustrated using a control problem from the Active Control Technique Evaluation for Spacecraft (ACES) testbed at NASA Marshall Space Flight Center in Huntsville, Alabama. A useful feature of maximum entropy design, seen in the example, is that it often produces controllers that are effectively reduced-order controllers. Other features of maximum entropy controllers are described in Refs. 6 and 7.

The paper is organized as follows. Section II develops the maximum entropy design equations. Section III gives a brief synopsis of homotopy methods. Next, Sec. IV develops a new

Received Oct. 21, 1992; revision received June 18, 1993; accepted for publication June 19, 1993.

*Staff Engineer, Government Aerospace Systems Division, MS 22/4849.

†Associate Principal Engineer, Government Aerospace Systems Division, MS 22/4849.

homotopy algorithm for maximum entropy control design. Section V illustrates the algorithm using a 17th-order model of one of the transfer functions of the ACES structure at NASA Marshall Space Flight Center. Finally, Sec. VI discusses the conclusions.

II. Maximum Entropy Design Equations

Consider the system

$$\dot{x}(t) = Ax(t) + Bu(t) + w_1(t)$$

$$y(t) = Cx(t) + Du(t) + w_2(t)$$

where $x \in \mathbb{R}^{n_x}$, $u \in \mathbb{R}^{n_u}$, $y \in \mathbb{R}^{n_y}$, $w_1 \in \mathbb{R}^{n_x}$ is white disturbance noise with intensity $V_1 \geq 0$, $w_2 \in \mathbb{R}^{n_y}$ is white observation noise with intensity $V_2 > 0$, and w_1 and w_2 have cross correlation $V_{12} \in \mathbb{R}^{n_x \times n_y}$. It is assumed that (A, B) is stabilizable and (A, C) is detectable. Also, the matrix A is assumed to be of the form

$$A = \text{block diag}[A^{(1)}, A^{(2)}]$$

where $A^{(2)}$ represents the dynamics that are certain and $A^{(1)}$ represents the nominal dynamics of the uncertain modes and is in real normal form; for example,

$$A^{(1)} = \text{block diag}\left\{\begin{bmatrix} -\nu_1 & \omega_1 \\ -\omega_1 & -\nu_1 \end{bmatrix}, \quad -\nu_2, \quad \begin{bmatrix} -\nu_3 & \omega_3 \\ -\omega_3 & -\nu_3 \end{bmatrix}\right\}$$

We also assume that only the modes with complex eigenvalues, corresponding to the 2×2 blocks

$$\begin{bmatrix} -\nu_j & \omega_j \\ -\omega_j & -\nu_j \end{bmatrix}$$

are uncertain and that the uncertainty patterns $A_i \in \mathbb{R}^{n_x \times n_x}$ are of the form

$$A_i = \text{block diag}\left\{0, \ldots, 0, \quad \begin{bmatrix} 0 & 1 \\ -1 & 0 \end{bmatrix}, \quad 0, \ldots, 0\right\}$$

Notice that the A_i correspond to errors in the undamped natural frequencies, i.e., the imaginary part of the eigenvalues.

The maximum entropy control design problem is stated as follows. Find a full-order dynamic compensator (i.e., a compensator of order n_x),

$$\dot{x}_c(t) = A_c x_c(t) + B_c y(t)$$

$$u(t) = -C_c x_c(t)$$

which stabilizes $\tilde{A}_s$, defined later, and minimizes the cost functional

$$J(A_c, B_c, C_c) = \text{tr}\, \tilde{Q}\tilde{R}$$

where $\tilde{Q}$ satisfies

$$0 = \tilde{A}_s\tilde{Q} + \tilde{Q}\tilde{A}_s^T + \tilde{V} + \sum_{i=1}^{n_\alpha} \tilde{A}_i\tilde{Q}\tilde{A}_i^T$$

and

$$\tilde{A}_s = \tilde{A} + \frac{1}{2}\sum_{i=1}^{n_\alpha} \alpha_i^2 \tilde{A}_i^2, \qquad \tilde{A}_i = \text{block diag}\{A_i, 0_{n_x}\}$$

$$\tilde{A} = \begin{bmatrix} A & -BC_c \\ B_cC & A_c - B_cDC_c \end{bmatrix}$$

$$\tilde{R} = \begin{bmatrix} R_1 & R_{12}C_c \\ C_c^TR_{12}^T & C_c^TR_2C_c \end{bmatrix}, \quad \tilde{V} = \begin{bmatrix} V_1 & V_{12}B_c^T \\ B_cV_{12}^T & B_cV_2B_c^T \end{bmatrix}$$

There is currently no rigorous justification for the requirement that $\tilde{A}_s$ be stabilized, but extensive numerical examples have shown that stability of $\tilde{A}_s$ insures stability of the nominal closed-loop system. Notice that if no uncertainty is assumed (i.e., $\alpha_i \triangleq 0$), then the maximum entropy control design problem becomes the standard LQG problem. The solution to the maximum entropy problem is characterized by the following theorem.

Theorem 1[3-5]. Suppose (A_c, B_c, C_c) solves the maximum entropy control design problem. Then, there exist nonnegative-definite matrices Q, P, $\hat{Q}$, and $\hat{P}$ such that A_c, B_c, and C_c are given by

$$A_c = A_s - BR_2^{-1}P_a - Q_aV_2^{-1}C + Q_aV_2^{-1}DR_2^{-1}P_a$$

$$B_c = Q_aV_2^{-1}, \qquad C_c = R_2^{-1}P_a$$

where

$$A_s = A + \frac{1}{2}\sum_{i=1}^{n_\alpha} \alpha_i^2 A_i^2$$

$$P_a = B^TP + R_{12}^T, \qquad Q_a = QC^T + V_{12}$$

and the following conditions are satisfied:

$$0 = A_s^TP + PA_s + R_1 - P_a^TR_2^{-1}P_a + \sum_{i=1}^{n_\alpha} \alpha_i^2 A_i^T(P + \hat{P})A_i \quad (1)$$

$$0 = A_sQ + QA_s^T + V_1 - Q_aV_2^{-1}Q_a^T + \sum_{i=1}^{n_\alpha} \alpha_i^2 A_i(Q + \hat{Q})A_i^T \quad (2)$$

$$0 = (A_s - Q_aV_2^{-1}C)^T\hat{P} + \hat{P}(A_s - Q_aV_2^{-1}C) + P_a^TR_2^{-1}P_a \quad (3)$$

$$0 = (A_s - BR_2^{-1}P_a)\hat{Q} + \hat{Q}(A_s - BR_2^{-1}P_a)^T + Q_aV_2^{-1}Q_a^T \quad (4)$$

Remark 1. If no uncertainty is assumed (i.e., $\alpha_i \triangleq 0$), then Eqs. (1-4) decouple, Eqs. (1) and (2) become the standard LQG regulator and estimator Riccati equations, and (A_c, B_c, C_c) defined in Theorem 1 is an LQG compensator.

III. Homotopy Methods for the Solution of Nonlinear Algebraic Equations

In the next section, we present a homotopy algorithm for solving the maximum entropy design equations (1-4). A homotopy is a continuous deformation of one function into another. The purpose of this section is to provide a very brief description of homotopy methods for finding the solutions of nonlinear algebraic equations. The reader is referred to Refs. 15-17 for additional details.

The basic problem is as follows. Given set Θ and Φ contained in $\mathbb{R}^n$ and a mapping $F: \Theta \rightarrow \Phi$, find solutions to

$$F(\theta) = 0$$

Homotopy methods embed the problem $F(\theta) = 0$ in a larger problem. In particular, let $H: \Theta \times [0, 1] \rightarrow \mathbb{R}^n$ be such that the following conditions exist:

1) $H(\theta, 1) = F(\theta)$.

2) There exists at least one known $\theta_0 \in \mathbb{R}^n$ that is a solution to $H(\cdot, 0) = 0$, i.e.,

$$H(\theta_0, 0) = 0$$

3) There exists a continuous curve $(\theta(\lambda), \lambda)$ in $\mathbb{R}^n \times [0, 1]$ such that

$$H(\theta(\lambda), \lambda) = 0 \quad \text{for} \quad \lambda \in [0, 1]$$

with

$$(\theta(0), 0) = (\theta_0, 0)$$

4) The curve $(\theta(\lambda), \lambda)$ is differentiable.

A homotopy algorithm then constructs a procedure to compute the actual curve $(\theta(\lambda), \lambda)$ such that the initial solution $\theta(0)$ is transformed to a desired solution $\theta(1)$ satisfying

$$0 = H(\theta(1), 1) = F(\theta(1))$$

Differentiating $H(\theta(\lambda), \lambda) = 0$ with respect to λ yields Davidenko's differential equation:

$$\frac{\partial H}{\partial \theta}\frac{\mathrm{d}\theta}{\mathrm{d}\lambda} + \frac{\partial H}{\partial \lambda} = 0 \tag{5}$$

Together with $\theta(0) = \theta_0$, Eq. (5) defines an initial value problem that by numerical integration from 0 to 1 yields the desired solution $\theta(1)$. Some numerical integration schemes are described in Ref. 17.

IV. Homotopy Algorithm for Full-Order Maximum Entropy Control Design

This section presents a novel homotopy algorithm that can be used to design full-order maximum entropy controllers. The algorithm is based on explicitly solving the four coupled maximum entropy design equations given in Eqs. (1–4).

A. Homotopy Map

To define the homotopy map we assume that the plant matrices (A, B, C, D), the cost-weighting matrices (R_1, R_2, R_{12}), the disturbance matrices (V_1, V_2, V_{12}), and the vector of uncertainty weights ($\alpha \in \Re^{n_\alpha}$) are functions of the homotopy parameter $\lambda \in [0, 1]$. In particular, the following is assumed:

$$\begin{bmatrix} A(\lambda) & B(\lambda) \\ C(\lambda) & D(\lambda) \end{bmatrix} = \begin{bmatrix} A_0 & B_0 \\ C_0 & D_0 \end{bmatrix} + \lambda\left\{\begin{bmatrix} A_f & B_f \\ C_f & D_f \end{bmatrix} - \begin{bmatrix} A_0 & B_0 \\ C_0 & D_0 \end{bmatrix}\right\}$$

$$\begin{bmatrix} R_1(\lambda) & R_{12}(\lambda) \\ R_{12}^T(\lambda) & R_2(\lambda) \end{bmatrix} = L_R(\lambda)L_R^T(\lambda)$$

where

$$L_R(\lambda) = L_{R,0} + \lambda(L_{R,f} - L_{R,0})$$

and $L_{R,0}$ and $L_{R,f}$ satisfy

$$L_{R,0}L_{R,0}^T \triangleq \begin{bmatrix} R_{1,0} & R_{12,0} \\ R_{12,0}^T & R_{2,0} \end{bmatrix}, \qquad L_{R,f}L_{R,f}^T \triangleq \begin{bmatrix} R_{1,f} & R_{12,f} \\ R_{12,f}^T & R_{2,f} \end{bmatrix}$$

$$\begin{bmatrix} V_1(\lambda) & V_{12}(\lambda) \\ V_{12}^T(\lambda) & V_2^T(\lambda) \end{bmatrix} = L_V(\lambda)L_V^T(\lambda)$$

where

$$L_V(\lambda) = L_{V,0} + \lambda(L_{V,f} - L_{V,0})$$

and $L_{V,0}$ and $L_{V,f}$ satisfy

$$L_{V,0}L_{V,0}^T = \begin{bmatrix} V_{1,0} & V_{12,0} \\ V_{12,0}^T & V_{2,0} \end{bmatrix}, \qquad L_{V,f}L_{V,f}^T = \begin{bmatrix} V_{1,f} & V_{12,f} \\ V_{12,f}^T & V_{2,0} \end{bmatrix}$$

$$\alpha_i^2(\lambda) = \alpha_{0,i}^2 + \lambda(\alpha_{f,i}^2 - \alpha_{0,i}^2), \qquad i = 1, 2, \ldots, n_\alpha$$

Notice that at $\lambda = 0$, $A(\lambda) = A_0$, $B(\lambda) = B_0, \ldots, \alpha_i^2(\lambda) = \alpha_{0,i}^2$, whereas at $\lambda = 1$, $A(\lambda) = A_f$, $B(\lambda) = B_f, \ldots, \alpha_i^2(\lambda) = \alpha_{f,i}^2$. Some guidelines for choosing the initial and final matrices are discussed later in Sec. IV.C.

The homotopy $0 = H((P, Q, \hat{P}, \hat{Q}), \lambda)$ is given by the equations

$$0 = A_s(\lambda)^T P(\lambda) + P(\lambda)A_s(\lambda) + R_1(\lambda) - P_a(\lambda)^T R_2(\lambda)^{-1} P_a(\lambda) + \sum_{i=1}^{n_\alpha} \alpha_i^2(\lambda) A_i^T P(\lambda) A_i + \sum_{i=1}^{n_\alpha} \alpha_i^2(\lambda) A_i^T \hat{P}(\lambda) A_i \tag{6}$$

$$0 = A_s(\lambda)Q(\lambda) + Q(\lambda)A_s(\lambda)^T + V_1(\lambda) - Q_a(\lambda)V_2^{-1}(\lambda)Q_a(\lambda)^T + \sum_{i=1}^{n_\alpha} \alpha_i^2(\lambda) A_i Q(\lambda) A_i^T + \sum_{i=1}^{n_\alpha} \alpha_i^2 A_i \hat{Q}(\lambda) A_i^T \tag{7}$$

$$0 = \left[A_s(\lambda) - Q_a(\lambda)V_2^{-1}(\lambda)C(\lambda)\right]^T \hat{P}(\lambda) + \hat{P}(\lambda)\left[A_s(\lambda) - Q_a(\lambda)V_2^{-1}(\lambda)C(\lambda)\right] + P_a(\lambda)^T R_2^{-1}(\lambda) P_a(\lambda) \tag{8}$$

$$0 = \left[A_s(\lambda) - B(\lambda)R_2^{-1}(\lambda)P_a(\lambda)\right]\hat{Q}(\lambda) + \hat{Q}(\lambda)\left[A_s(\lambda) - B(\lambda)R_2^{-1}(\lambda)P_a(\lambda)\right]^T + Q_a(\lambda)V_2^{-1}(\lambda)Q_a(\lambda)^T \tag{9}$$

where

$$A_s(\lambda) \triangleq A(\lambda) + \frac{1}{2}\sum_{i=1}^{n_\alpha} \alpha_i^2(\lambda) A_i^2$$

$$P_a(\lambda) \triangleq B(\lambda)^T P(\lambda) + R_{12}(\lambda)^T, \qquad Q_a(\lambda) \triangleq Q(\lambda)C(\lambda)^T + V_{12}(\lambda)$$

B. Derivative and Correction Equations

The homotopy algorithm presented in the next section uses a predictor/corrector numerical integration scheme. The predictor steps require derivatives $[\dot{P}(\lambda), \dot{Q}(\lambda), \dot{\hat{P}}(\lambda)\ \dot{\hat{Q}}(\lambda)]$, where $\dot{M} \triangleq \mathrm{d}M/\mathrm{d}\lambda$, whereas the correction step is based on using Newton corrections, denoted here as $(\Delta P, \Delta Q, \Delta\hat{P}, \Delta\hat{Q})$. Next we derive the matrix equations that can be used to solve for the derivatives and corrections. For notational simplicity we omit the argument λ in the derived equations.

1. Derivative Equations

Differentiating Eqs. (6–9) with respect to λ gives the following coupled matrix equations:

$$0 = A_P^T \dot{P} + \dot{P}A_P + R + \sum_{i=1}^{n_\alpha} \alpha_i^2 A_i^T \dot{P} A_i + \sum_{i=1}^{n_\alpha} \alpha_i^2 A_i^T \dot{\hat{P}} A_i \tag{10}$$

$$0 = A_Q \dot{Q} + \dot{Q}A_Q^T + V + \sum_{i=1}^{n_\alpha} \alpha_i^2 A_i \dot{Q} A_i^T + \sum_{i=1}^{n_\alpha} \alpha_i^2 A_i \dot{\hat{Q}} A_i^T \tag{11}$$

$$0 = A_Q^T \dot{\hat{P}} + \dot{\hat{P}} A_Q + \hat{R} + G_C \dot{Q}\hat{F} + \hat{F}\dot{Q}G_C + H_P^T \dot{P} K_P + K_P^T \dot{P} H_P \tag{12}$$

$$0 = A_P \dot{\hat{Q}} + \dot{\hat{Q}} A_P^T + \hat{V} + G_B \dot{P}\hat{E} + \hat{E}\dot{P}G_B + H_Q \dot{Q} K_Q^T + K_Q \dot{Q} H_Q^T \tag{13}$$

where

$$A_P \triangleq A_s - BR_{2,\mathrm{inv}}P_a, \qquad A_Q \triangleq A_s - Q_a V_{2,\mathrm{inv}} C$$

$$R \triangleq \dot{A}_s^T P + P\dot{A}_s + \dot{R}_1 - P_a^T R_{2,\mathrm{inv}}(\dot{B}^T P + \dot{R}_{12}^T) - (P\dot{B} + \dot{R}_{12})R_{2,\mathrm{inv}}P_a - P_a^T \dot{R}_{2,\mathrm{inv}} P_a + \sum_{i=1}^{n_\alpha} \dot{\alpha}_{i,\mathrm{sq}} A_i^T (P + \hat{P}) A_i$$

$$V \triangleq \dot{A}_s Q + Q\dot{A}_s^T + \dot{V}_1 - Q_a V_{2,\mathrm{inv}}(\dot{C}Q + \dot{V}_{12}^T) - (Q\dot{C}^T + \dot{V}_{12})V_{2,\mathrm{inv}}Q_a^T - Q_a \dot{V}_{2,\mathrm{inv}} Q_a^T + \sum_{i=1}^{n_\alpha} \dot{\alpha}_{i,\mathrm{sq}} A_i (Q + \hat{Q}) A_i^T$$

$$\hat{R} \triangleq \left[\dot{A}_s - Q_a V_{2,\text{inv}}\dot{C} - Q_a \dot{V}_{2,\text{inv}} C - (Q\dot{C}^T + \dot{V}_{12})V_{2,\text{inv}} C\right]^T \hat{P}$$
$$+ \hat{P}\left[\dot{A}_s - Q_a V_{2,\text{inv}}\dot{C} - Q_a \dot{V}_{2,\text{inv}} C - (Q\dot{C}^T + \dot{V}_{12})V_{2,\text{inv}} C\right]$$
$$+ P_a^T R_{2,\text{inv}}(\dot{B}^T P + \dot{R}_{12}^T) + (\dot{B}^T P + \dot{R}_{12}^T)^T R_{2,\text{inv}} P_a$$
$$+ P_a^T \dot{R}_{2,\text{inv}} P_a$$

$$\hat{V} \triangleq \left[\dot{A}_s - \dot{B}R_{2,\text{inv}}P_a - B\dot{R}_{2,\text{inv}}P_a - BR_{2,\text{inv}}(\dot{B}^T P + \dot{R}_{12}^T)\right]\hat{Q}$$
$$+ \hat{Q}\left[\dot{A}_s - \dot{B}R_{2,\text{inv}}P_a - B\dot{R}_{2,\text{inv}}P_a - BR_{2,\text{inv}}(\dot{B}^T P + \dot{R}_{12}^T)\right]^T$$
$$+ Q_a V_{2,\text{inv}}(Q\dot{C}^T + \dot{V}_{12})^T + (Q\dot{C}^T + \dot{V}_{12})V_{2,\text{inv}} Q_a^T$$
$$+ Q_a \dot{V}_{2,\text{inv}} Q_a^T$$

$$G_B = -BR_{2,\text{inv}}B^T, \quad G_c = -C^T V_{2,\text{inv}} C, \quad \hat{E} = \hat{Q}, \quad \hat{F} = \hat{P}$$

$$H_P = BR_{2,\text{inv}}P_a, \quad H_Q = Q_a V_{2,\text{inv}} C, \quad K_P = I_{n_x}, \quad K_Q = I_{n_x}$$

Note that in the previous equations we have used the notations

$$R_{2,\text{inv}} \triangleq R_2^{-1}, \qquad V_{2,\text{inv}} \triangleq V_2^{-1}, \qquad \alpha_{i,\text{sq}} \triangleq \alpha_i^2$$

2. Correction Equations

The correction equations are developed with λ at some fixed value, say λ^*. The derivation of the correction equations is based on the relationship between Newton's method and a particular homotopy. In the following text we use the notation

$$f'(\theta) \triangleq \frac{\partial f}{\partial \theta}$$

Let $f : \mathbb{R}^n \to \mathbb{R}^n$ be C^1 and consider the equation

$$0 = f(\theta) \tag{14}$$

If $\theta^{(i)}$ is the current approximation to the solution of Eq. (14), then the Newton correction[18] $\Delta\theta$ is given by

$$\theta^{(i+1)} - \theta^{(i)} \triangleq \Delta\theta = -f'(\theta^{(i)})^{-1} e \tag{15}$$

where

$$e \triangleq f(\theta^{(i)})$$

Now, let $\theta^{(i)}$ be an approximation to θ satisfying Eq. (14). Then, with e as given immediately above, construct the following homotopy to solve Eq. (14):

$$(1-\beta)e = f\big(\theta(\beta)\big), \qquad \beta \in [0, 1] \tag{16}$$

[Note that at $\beta = 0$ Eq. (16) has solution $\theta(0) = \theta^{(i)}$, whereas $\theta(1)$ satisfies Eq. (14)]. Then, differentiating Eq. (16) with respect to β gives

$$\left.\frac{\partial \theta}{\partial \beta}\right|_{\beta=0} = -f'(\theta^{(i)})^{-1} e \tag{17}$$

Remark 2. Note that the Newton correction $\Delta\theta$ in Eq. (15) and the derivative $\partial\theta/\partial\beta|_{\beta=0}$ in Eq. (17) are identical. Hence, the Newton correction $\Delta\theta$ can be found by constructing a homotopy of the form of Eq. (16) and solving for the resulting derivative $\partial\theta/\partial\beta|_{\beta=0}$. As seen later, this insight is particularly useful when deriving Newton corrections for equations that have a matrix structure. It is also of interest to note that the homotopy of Eq. (16) is appropriately referred to in some literature as a "Newton homotopy."[15]

Now, we use the insights of Remark 2 to derive the equations that need to be solved for the Newton corrections (ΔP, ΔQ, $\Delta\hat{P}$, $\Delta\hat{Q}$). We begin by recalling that λ is assumed to have some fixed value, say λ^*. Also, it is assumed that P^*, Q^*, $\hat{P}^*$, and $\hat{Q}^*$ are the current approximations to $P(\lambda^*)$, $Q(\lambda^*)$, $\hat{P}(\lambda^*)$, and $\hat{Q}(\lambda^*)$ and that E_P, E_Q, $E_{\hat{P}}$, and $E_{\hat{Q}}$ are, respectively, the errors in Eqs. (1-4) with $\lambda = \lambda^*$ and $P(\lambda)$, $Q(\lambda)$, $\hat{P}(\lambda)$, and $\hat{Q}(\lambda)$ replaced by P^*, Q^*, $\hat{P}^*$, and $\hat{Q}^*$.

We next form the homotopy

$$(1-\beta)E_P = A_s^T P(\beta) + P(\beta)A_s + R_1 - P_a(\beta)^T R_2^{-1} P_a(\beta)$$
$$+ \sum_{i=1}^{n_\alpha} \alpha_i^2 A_i^T P(\beta) A_i + \sum_{i=1}^{n_\alpha} \alpha_i^2 A_i^T \hat{P}(\beta) A_i \tag{18}$$

$$(1-\beta)E_Q = A_s Q(\beta) + Q(\beta)A_s^T + V_1 - Q_a(\beta)V_2^{-1} Q_a(\beta)^T$$
$$+ \sum_{i=1}^{n_\alpha} \alpha_i^2 A_i Q(\beta) A_i^T + \sum_{i=1}^{n_\alpha} \alpha_i^2 A_i \hat{Q}(\beta) A_i^T \tag{19}$$

$$(1-\beta)E_{\hat{P}} = \left[A_s Q_a(\beta)V_2^{-1} C\right]^T \hat{P}(\beta)$$
$$+ \hat{P}(\beta)\left[A_s - Q_a(\beta)V_2^{-1} C\right] + P_a(\beta)^T R_2^{-1} P_a(\beta) \tag{20}$$

$$(1-\beta)E_{\hat{Q}} = \left[A_s - BR_2^{-1} P_a(\beta)\right]\hat{Q}(\beta)$$
$$+ \hat{Q}(\beta)\left[A_s - BR_2^{-1} P_a(\beta)\right]^T + Q_a(\beta)V_2^{-1} Q_a(\beta)^T \tag{21}$$

where

$$A_s = A + \sum_{i=1}^{n_\alpha} \alpha_i^2 A_i^2$$

$$P_a = B^T P(\beta) + R_{12}^T, \qquad Q_a = Q(\beta)C^T + V_{12}$$

and the system matrices are assumed to be evaluated at $\lambda = \lambda^*$, i.e., $(A, B, \ldots, R_1, R_2, \ldots) = [A(\lambda^*), B(\lambda^*), \ldots, R_1(\lambda^*), R_2(\lambda^*), \ldots]$. Differentiating Eqs. (18-21) with respect to β and using Remark 4 to make the replacements

$$\Delta P = \left.\frac{\mathrm{d}P}{\mathrm{d}\beta}\right|_{\beta=0}, \qquad \Delta Q = \left.\frac{\mathrm{d}Q}{\mathrm{d}\beta}\right|_{\beta=0}$$
$$\Delta \hat{P} = \left.\frac{\mathrm{d}\hat{P}}{\mathrm{d}\beta}\right|_{\beta=0}, \qquad \Delta \hat{Q} = \left.\frac{\mathrm{d}\hat{Q}}{\mathrm{d}\beta}\right|_{\beta=0}$$

gives

$$0 = A_P^T \Delta P + \Delta P A_P + R + \sum_{i=1}^{n_\alpha} \alpha_i^2 A_i^T \Delta P A_i$$
$$+ \sum_{i=1}^{n_\alpha} \alpha_i^2 A_i^T \Delta\hat{P} A_i \tag{22}$$

$$0 = A_Q \Delta Q + \Delta Q A_Q^T + V + \sum_{i=1}^{n_\alpha} \alpha_i^2 A_i \Delta Q A_i^T$$
$$+ \sum_{i=1}^{n_\alpha} \alpha_i^2 A_i \Delta\hat{Q} A_i^T \tag{23}$$

$$0 = A_Q^T \Delta\hat{P} + \Delta\hat{P} A_Q + \hat{R} + G_C \Delta Q \hat{F} + \hat{F}\Delta Q G_C$$
$$+ H_P^T \Delta P K_P + K_P^T \Delta P H_P \tag{24}$$

$$0 = A_P \Delta\hat{Q} + \Delta\hat{Q} A_P^T + \hat{V} + G_B \Delta P \hat{E} + \hat{E}\Delta P G_B$$
$$+ H_Q \Delta Q K_Q^T + K_Q \Delta Q H_Q^T \tag{25}$$

where

$$A_P \triangleq A_s - BR_2^{-1} P_a, \qquad A_Q \triangleq A_s - Q_a V_2^{-1} C$$

$$R = E_P, \qquad V = E_Q, \qquad \hat{R} = E_{\hat{P}}, \qquad \hat{V} = E_{\hat{Q}}$$

$$G_B = -BR_2^{-1} B^T, \quad G_c = -C^T V_2^{-1} C, \quad \hat{E} = \hat{Q}, \quad \hat{F} = \hat{P}$$

$$H_P = BR_2^{-1} P_a, \quad H_Q = Q_a V_2^{-1} C, \quad K_P = I_{n_x}, \quad K_Q = I_{n_x}$$

Comparing Eqs. (22-25) with Eqs. (10-13) reveals that the derivative and correction equations are identical in form. Each set of equations consists of four coupled Lyapunov equations. Since these equations are linear, by using Kronecker products[14] they can be converted to the vector form $\mathcal{C}\chi = b$ where for Eqs. (22-25) χ is a vector containing the independent elements of ΔP, ΔQ, $\Delta\hat{P}$, and $\Delta\hat{Q}$. The $\mathcal{C}$ is then a square matrix of dimension $2n_x(n_x+1)$. Inversion of $\mathcal{C}$ is hence very computationally intensive for even relatively small problems (e.g., $n_x = 10$).

Fortunately, the coupling terms described by the summation terms in Eqs. (22) and (23) are relatively sparse. In particular, each summation has only $3n_\alpha$ independent terms. Hence, a technique similar to that described in Ref. 19, which exploits this sparseness, can be used to efficiently solve Eqs. (22-25) [or equivalently Eqs. (10-13)]. The details of the solution procedure are described in Appendix B. The solution procedure relies on the solution of a maximum entropy Lyapunov equation as described in Appendix A. The results of Appendix A are also based on the results of Ref. 19. Both Appendices A and B rely on diagonalization of the coefficient matrices of each of the Lyapunov equations. Since efficient MATLAB implementation requires the minimization of the use of *for loops*, the solution procedures of Appendices A and B implement the techniques of Ref. 19 with minimal looping. A complete derivation of these results is presented in Ref. 20.

C. Overview of the Homotopy Algorithm

This section describes the general logic and features of the homotopy algorithm for full-order maximum entropy control. It is assumed that the designer has supplied a set of system matrices $S_f = (A_f, B_f, C_f, D_f, R_{1,f}, R_{2,f}, R_{12,f}, V_{1,f}, V_{2,f}, V_{12,f}, \alpha_f)$ describing the optimization problem whose solution is desired. In addition, it is assumed that the designer has chosen an initial set of related system matrices $S_0 = (A_0, B_0, C_0, D_0, R_{1,0}, R_{2,0}, R_{12,0}, V_{1,0}, V_{2,0}, V_{1,0}, \alpha_0)$ that has an easily obtained or known solution $(P_0, Q_0 \hat{P}_0, \hat{Q}_0)$ to the maximum entropy design equations. Note that we can always choose $\alpha_0 = 0$ in which case $(P_0, Q_0, \hat{P}_0, \hat{Q}_0)$ corresponds to an LQG problem and can be computed using standard Riccati equation and Lyapunov equation solvers. In practice, we often choose the remaining system matrices to have equal initial and final values, i.e., $A_f = A_0$, $B_f = B_0$, $\ldots, R_{1,f} = R_{1,0}$, $R_{2,f} = R_{2,0}, \ldots, V_{1,f} = V_{1,0}$, $V_{2,f} = V_{2,0}$. However, there is a strong rationale for allowing these matrices to vary during the homotopy. For example, suppose a maximum entropy controller of a particular robustness (corresponding to some value of α) is designed but the controller authority level is not desirable. Then, instead of changing the weights $R_1, R_2, R_{12}, V_1, V_2$, and V_{12} to reflect the desired authority level, solving the corresponding LQG problem (that is, the problem with $\alpha = 0$), and then using the homotopy algorithm to reinsert the robustness (corresponding to the original value of α), we can use the homotopy algorithm to modify the weights $R_1, R_2, \ldots$, with α fixed to its original value. Similarly, we can modify the nominal plant matrices A, B, C, and D with α fixed to reflect new data concerning the plant.

Later we present an outline of the homotopy algorithm. This algorithm describes a predictor/corrector numerical integration scheme. The prediction step uses cubic spline prediction as described next.

1. Cubic Spline Prediction

Here we use the notation that λ_0, λ_{-1}, and λ_1 represent the values of λ at, respectively, the current point on the homotopy curve, the previous point, and the next point. Also, $\dot{M} \triangleq \mathrm{d}M/\mathrm{d}\lambda$. The prediction of $P(\lambda_1)$ requires $P(\lambda_0)$, $\dot{P}(\lambda_0)$, $P(\lambda_{-1})$, and $\dot{P}(\lambda_{-1})$. In particular,

$$\operatorname{vec}\left[P(\lambda_1)\right] = a_0 + a_1\lambda_1 + a_2\lambda_1^2 + a_3\lambda_1^3$$

where a_0, a_1, a_2, and a_3 are computed by solving

$$[a_0\ a_1\ a_2\ a_3]\begin{bmatrix} 1 & 0 & 1 & 0 \\ \lambda_{-1} & 1 & \lambda_0 & 1 \\ \lambda_{-1}^2 & 2\lambda_{-1} & \lambda_0^2 & 2\lambda_0 \\ \lambda_{-1}^3 & 3\lambda_{-1}^2 & \lambda_0^3 & 3\lambda_0^2 \end{bmatrix} = \begin{Bmatrix} \operatorname{vec}\left[P(\lambda_{-1})\right] \\ \operatorname{vec}\left[\dot{P}(\lambda_{-1})\right] \\ \operatorname{vec}\left[P(\lambda_0)\right] \\ \operatorname{vec}\left[\dot{P}(\lambda_0)\right] \end{Bmatrix}$$

Note that if $P(\lambda_{-1})$ and $\dot{P}(\lambda_{-1})$ are not available (as occurs at the initial iteration of the homotopy algorithm), the $P(\lambda_1)$ is predicted using linear prediction, i.e.,

$$P(\lambda_1) = P(\lambda_0) + (\lambda_1 - \lambda_0)\dot{P}(\lambda_0)$$

2. Outline of the Homotopy Algorithm

Step 1: Initialize loop = 0, $\lambda = 0$, $\Delta\lambda \in [0, 1]$, $S = S_0$, $(P, Q, \hat{P}, \hat{Q}) = (P_0, Q_0, \hat{P}_0, \hat{Q}_0)$.

Step 2: Let loop = loop + 1. If loop = 1, then go to step 4.

Step 3: Advance the homotopy parameter λ and predict the corresponding $P(\lambda)$, $Q(\lambda)$, $\hat{P}(\lambda)$, and $\hat{Q}(\lambda)$ as follows:

3a: Let $\lambda_0 = \lambda$.

3b: Let $\lambda = \lambda_0 + \Delta\lambda$.

3c: Compute $\dot{P}(\lambda_0)$, $\dot{Q}(\lambda_0)$, $\dot{\hat{P}}(\lambda_0)$, and $\dot{\hat{Q}}(\lambda_0)$ using Eqs. (10-13).

3d: If loop = 2, predict $P(\lambda)$, $Q(\lambda)$, $\hat{P}(\lambda)$, and $\hat{Q}(\lambda)$ using linear prediction, or else predict $P(\lambda)$, $Q(\lambda)$, $\hat{P}(\lambda)$, and $\hat{Q}(\lambda)$ using cubic spline prediction.

3e: Compute the errors $(E_P, E_Q, E_{\hat{P}}, E_{\hat{Q}})$ in the maximum entropy equations (1-4). If the $\max(\|E_P\|, \|E_Q\|, \|E_{\hat{P}}\|, \|E_{\hat{Q}}\|)$ satisfies some preassigned tolerance, then continue. Otherwise reduce $\Delta\lambda$ and go to step 3b.

Step 4: Correct the current approximations $P(\lambda)$, $Q(\lambda)$, $\hat{P}(\lambda)$, and $\hat{Q}(\lambda)$ as follows.

4a: Compute the errors $(E_P, E_Q, E_{\hat{P}}, E_{\hat{Q}})$ in the maximum entropy equations (1-4).

4b: Solve Eqs. (22-25) for ΔP, ΔQ, $\Delta\hat{P}$, and $\Delta\hat{Q}$.

4c: Let

$$P(\lambda) \leftarrow P(\lambda) + \Delta P, \qquad Q(\lambda) \leftarrow Q(\lambda) + \Delta Q$$

$$\hat{P}(\lambda) \leftarrow \hat{P}(\lambda) + \Delta\hat{P}, \qquad \hat{Q}(\lambda) \leftarrow \hat{Q}(\lambda) + \Delta\hat{Q}$$

4d: Recompute the errors $(E_P, E_Q, E_{\hat{P}}, E_{\hat{Q}})$ in the maximum entropy equations (1-4). If the $\max(\|E_P\|, \|E_Q\|, \|E_{\hat{P}}\|, \|E_{\hat{Q}}\|)$ satisfies some preassigned tolerance, then continue. Otherwise go to step 4b.

Step 5: If $\lambda = 1$, then stop. Otherwise go to step 2.

Remark 3. Since the corrections of step 4 correspond to Newton corrections, quadratic convergence can be insured by choosing the prediction tolerance, used in step 3e, sufficiently small. This insures that along the homotopy curve the approximation to $(P(\lambda), Q(\lambda), \hat{P}(\lambda), \hat{Q}(\lambda))$ is close to the optimal value $(P^*(\lambda), Q^*(\lambda), \hat{P}^*(\lambda), \hat{Q}^*(\lambda))$. Hence, the quadratic convergence properties of Newton's method[18] can be realized. This quadratic convergence has been observed in numerous examples.

Remark 4. The previous homotopy algorithm for maximum entropy design advanced the P and Q equations separately from the $\hat{P}$ and $\hat{Q}$ equations. That is, $P(\lambda)$ and $Q(\lambda)$ were corrected with $\hat{P}(\lambda) = \hat{P}_a(\lambda)$ and $\hat{Q}(\lambda) = \hat{Q}_a(\lambda)$ where $\hat{P}_a(\lambda)$ and $\hat{Q}_a(\lambda)$ are approximations. Similarly, $\hat{P}(\lambda)$ and $\hat{Q}(\lambda)$ were corrected with $P(\lambda) = P_a(\lambda)$ and $Q(\lambda) = Q_a(\lambda)$ where $P_a(\lambda)$ and $Q_a(\lambda)$ are approximations. This iterative scheme tends to converge slowly as the uncertainty level is increased and never exhibits quadratic convergence, no matter how small the prediction tolerance.

Notice that the algorithm relies on solving four coupled Lyapunov equations (10-13) or (22-25) at each prediction step or correction iteration. Efficient solution of these equations makes the algorithm feasible for large-scale systems. The current solution procedure is based on diagonalizing the coefficient matrices A_p and A_q of the coupled Lyapunov equations. This is usually possible. However, it is possible that this diag-

Table 1 Run-time statistics of the maximum entropy homotopy algorithm

Initial β	Final β	Megaflops	Real time, s	Predictions and corrections
0	0.01	1246	609	43
0.01	0.1	1062	519	36
0.1	1	1062	513	36
1	5	1212	617	41

Table 2 Robustness to simultaneous shifts in the undamped natural frequencies

β	$\Delta\omega_{\min}$, rad/s	$\Delta\omega_{\max}$, rad/s
0 (=LQG)	−0.000075	0.0075
0.01	−0.0037	0.036
0.1	−0.080	0.69
1	−1.6	7.1
5	−15	94

onalization will be intractable for some points along the homotopy path. In this case, one could randomly perturb the system matrices so that diagonalization is possible. The perturbation is then removed at the end of the homotopy curve. This type of random perturbation is commonly used in "probability one homotopies."[17] An alternative is to embed a numerical conditioning test in the program to determine whether the coefficient matrices are truly diagonalizable. If they are not, then one can solve the coupled Lyapunov equations using a nondiagonal alternative such as the Schur decomposition.

V. Illustration of Maximum Entropy Design Using the ACES Structure

This section illustrates the design of a maximum entropy controller for a 17th-order model of one of the single-input/single-output (SISO) transfer functions of the ACES structure at NASA Marshall Space Flight Center.[21] The actuator and sensor are, respectively, a torque actuator and a collocated rate gyro. The model includes the actuator and sensor dynamics. A first-order all-pass filter was appended to the model to approximate the computational delay associated with digital implementation.

The Bode plots of the open-loop plant are illustrated in Fig. 1. The basic control objective is to provide damping to the lower frequency modes of the structure (i.e., the modes less than 3 Hz) as measured by the rate gyro. The undamped natural frequencies of each of the eight flexible modes are considered uncertain. (Note that there are two modes at 2.4 Hz, one of which is virtually unobservable.) Maximum entropy design is used to add uncertainty to each of these modal frequencies to increase the design robustness. The uncertainty vector $\alpha \in \mathbb{R}^8$ is given by

$$\alpha = \beta * \alpha_0$$

where each element of $\alpha_0 \in \mathbb{R}^8$ has unity value, reflecting equal uncertainty in each of the flexible modes and β is a scale factor chosen to represent the level of uncertainty. The precise relationship between β and the allowable frequency perturbations is not currently defined by maximum entropy theory.

For this example, the MATLAB implementation of the maximum entropy homotopy algorithm was run on a 486, 66-MHz personal computer. The only system matrix that was allowed to vary was α; hence, $A_f = A_0$, $B_f = B_0, \ldots, V_{12,f} = V_{12,0}$. Table 1 shows some of the run-time statistics of the program. The highest uncertainty design, corresponding to $\beta = 5$, was obtained in approximately 37 min. Notice that the number of flops and the run time are essentially linear with respect to the log of the scale factor β. This general trend has also been observed in other design examples.

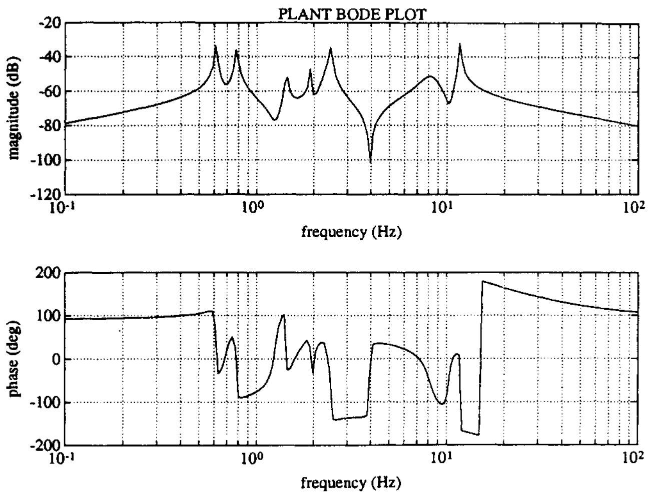

Fig. 1 Bode plot of SISO ACES transfer function.

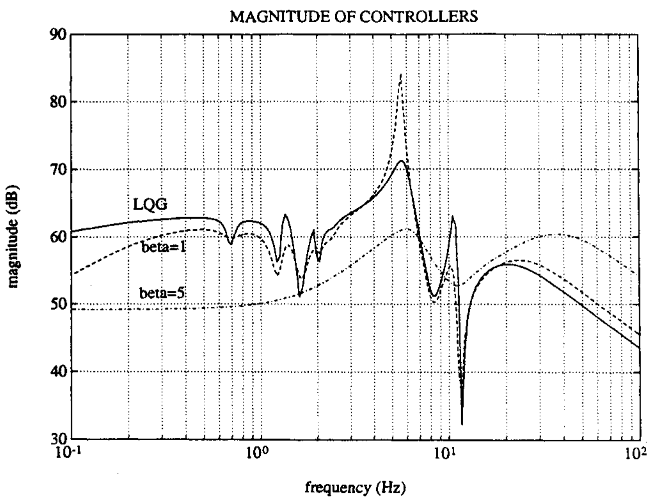

Fig. 2 Magnitude frequency response of LQG and maximum entropy controllers.

As β was increased, the maximum entropy controllers became increasingly more tolerant to changes in the (undamped) natural frequencies. Table 2 describes the robustness properties of the closed-loop systems when the natural frequencies of the open-loop plant were simultaneously shifted by $\Delta\omega$. The parameter $\Delta\omega_{\min}$ corresponds to the maximum negative frequency shift, whereas $\Delta\omega_{\max}$ corresponds to the maximum positive frequency shift. Notice that the LQG controller is very sensitive to perturbations in the natural frequencies. The maximum entropy controller corresponding to $\beta = 5$ allowed maximum perturbations that were more than four orders of magnitude greater than those allowed by the LQG controller. Robustness analysis that allows independent variations in the modal frequencies can be performed fairly nonconservatively by using theory based on Popov analysis and parameter-dependent Lyapunov functions.[12] An illustration of the application of this theory is given in Ref. 22.

Figures 2 and 3 compare, respectively, the magnitude and phase of the initial LQG controller and the maximum entropy controllers corresponding to $\beta = 1$ and 5. Notice that the $\beta = 5$ controller has a very smooth frequency response and is positive real over a very large frequency band, giving it very significant robustness. The magnitudes of the closed-loop transfer functions corresponding to the LQG compensator and $\beta = 5$ maximum entropy compensator are shown in Fig. 4. As would be expected, the nominal performance (measured by the amount

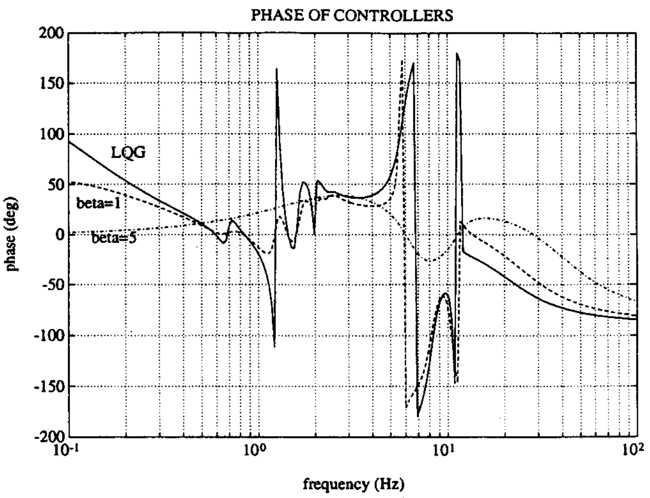

Fig. 3 Phase frequency responses of LQG and maximum entropy controllers.

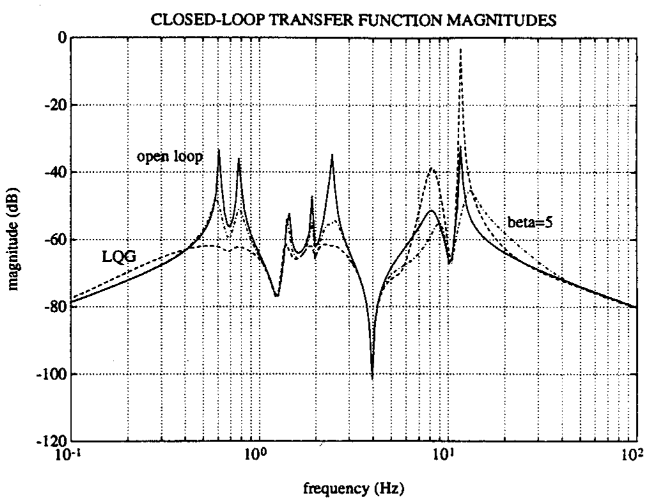

Fig. 4 Magnitude of the closed-loop transfer functions corresponding to the LQG and $\beta = 5$ maximum entropy controller.

of damping in the modes below 2 Hz) of the maximum entropy controller was significantly less than that provided by the LQG controller. However, significant damping was provided by this controller, and as previously discussed, this controller is much more robust than the LQG compensator.

The smoothness of the maximum entropy controller corresponding to $\beta = 5$ indicates that its effective order is much less than 17. Using balanced controller reduction,[23] a fourth-order compensator was obtained whose frequency response is nearly identical to that of the 17th-order compensator. The ability to produce what are essentially reduced-order controllers is an important practical feature of maximum entropy design. Another interesting feature of maximum entropy design is that it will sometimes widen and deepen controller notches to robustly gain stabilize certain modes. This property is illustrated in Refs. 6 and 7. In Ref. 8, maximum entropy design is applied to a multi-input/multi-output control problem, whereas in Ref. 10 maximum entropy design is applied to a neutrally stable system.

VI. Conclusions

This paper has presented a new homotopy algorithm for maximum entropy control design. The example of the previous section illustrated the use of the algorithm using a medium scale model (17 states) representing a transfer function of the ACES structure at NASA Marshall Space Flight Center. Very robust designs were obtained in a reasonable amount of time on a 66-MHz, 486 personal computer. For this example, an interesting feature of the most robust maximum entropy controller was that it was essentially a reduced-order controller. This allowed a 17th-order compensator to be easily reduced to a fourth-order compensator by using balanced controller reduction. The frequency responses of the two controllers were essentially identical, indicating that the reduced-order controller maintained the robustness and performance properties of the full-order controller. Algorithms of the type described here should also prove effective in the solution of other sets of coupled Riccati and Lyapunov equations appearing in robust control theory.

Appendix A: Efficient Computation of the Solution to the Maximum Entropy Lyapunov Equation

The Appendix presents a solution procedure for efficiently solving for Q satisfying the $n \times n$ maximum entropy Lyapunov equation

$$0 = A_s Q + Q A_s^T + V + \sum_{i=1}^{n_\alpha} \alpha_i^2 A_i Q A_i^T \tag{A1}$$

where

$$A_i = e(\ell_\alpha(i)) e(\ell_\alpha(i)+1)^T - e(\ell_\alpha(i)+1) e(\ell_\alpha(i))^T \tag{A2}$$

where $\ell_\alpha \in \mathbb{R}^{n_\alpha}$ is a vector with distinct elements, each of which lies in the interval $[1 \;\; n]$, and $e : [1, 2, \ldots, n] \to \mathbb{R}^n$ is defined by

$$e_i(k) = \begin{cases} 0, & i \neq k \\ 1, & i = k \end{cases}$$

It is assumed that Eq. (A1) has a unique solution. The solution procedure also assumes that A is nondefective and is based on transforming A to a complex, diagonal matrix. Details of the derivation of the solution procedure are given in Ref. 20.

Let Ψ be the eigenvector matrix of A, such that

$$A = \Psi \Lambda \Psi^{-1}$$

where $\Lambda \in \mathbb{C}^{n \times n}$ is diagonal. Then premultiplying and postmultiplying Eq. (A1), respectively, by Ψ^{-1} and Ψ^{-H} yield

$$0 = \Lambda \bar{Q} + \bar{Q} \Lambda^* + \bar{V} + M(\bar{Q})$$

where

$$\bar{Q} \triangleq \Psi^{-1} Q \Psi^{-H}$$
$$\bar{V} \triangleq \Psi^{-1} V \Psi^{-H}, \qquad M(\bar{Q}) = \sum_{i=1}^{n_\alpha} M_i(\bar{Q}) \tag{A3}$$

and

$$M_i(\bar{Q}) \triangleq \alpha_i^2 \Psi^{-1} A_i \Psi \bar{Q} \Psi^H A_i^T \Psi^{-H}$$

The solution procedure relies on the following definitions:

$$\omega_n \triangleq \begin{bmatrix} 1 \\ 1 \\ \vdots \\ 1 \end{bmatrix}, \qquad (\omega_n \in \mathbb{R}^n); \qquad \lambda \triangleq [\Lambda_{11} \;\; \Lambda_{22} \;\; \cdots \;\; \Lambda_{nn}]^T$$

$$S \triangleq -\mathrm{diag}^{-1}(\lambda \omega_n^T + \omega_n \lambda^H) \tag{A4}$$

$$M_{Q,\alpha} \triangleq \left[M_{Q,\alpha}^{(1)} \;\; M_{Q,\alpha}^{(2)} \;\; M_{Q,\alpha}^{(3)} \right] \tag{A5}$$

where

$$M_{Q,\alpha}^{(1)} = \left(\omega_n \otimes \Psi^{-1}(:, \ell_\alpha)\right) * \left(\Psi^{-*}(:, \ell_\alpha) \otimes \omega_n\right)$$

$$M_{Q,\alpha}^{(2)} = \left(\omega_n \otimes \Psi^{-1}(:, \ell_\alpha + \omega_n)\right) * \left(\Psi^{-*}(:, \ell_\alpha + \omega_{n_\alpha}) \otimes \omega_n\right)$$

$$M_{Q,\alpha}^{(3)} = \left(\omega_n \otimes \Psi^{-1}(:, \ell_\alpha)\right) * \left(\Psi^{-*}(:, \ell_\alpha + \omega_{n_\alpha}) \otimes \omega_n\right) + \left(\omega_n \otimes \Psi^{-1}(:, \ell_\alpha + \omega_{n_\alpha})\right) * \left(\Psi^{-*}(:, \ell_\alpha) \otimes \omega_n\right)$$

where

$$N_{Q,\alpha} \triangleq \begin{bmatrix} N_{Q,\alpha}^{(1)} \\ N_{Q,\alpha}^{(2)} \\ N_{Q,\alpha}^{(3)} \end{bmatrix} \tag{A6}$$

where

$$N_{Q,\alpha}^{(1)} = \left((\alpha * \alpha)\omega_{n^2}^T\right) * \left[\left(\Psi^*(\ell_\alpha + \omega_{n_\alpha}, :) \otimes \omega_n^T\right) + \left(\omega_n^T \otimes \Psi(\ell_\alpha + \omega_{n_\alpha}, :)\right)\right]$$

$$N_{Q,\alpha}^{(2)} = \left((\alpha * \alpha)\omega_{n^2}^T\right) * \left[\left(\Psi^*(\ell_\alpha, :) \otimes \omega_n^T\right) + \left(\omega_n^T \otimes \Psi(\ell_\alpha, :)\right)\right]$$

$$N_{Q,\alpha}^{(3)} = -\left((\alpha * \alpha)\omega_{n^2}^T\right) * \left[\left(\Psi^*(\ell_\alpha + \omega_{n_\alpha}, :) \otimes \omega_n^T\right) + \left(\omega_n^T \otimes \Psi(\ell_\alpha, :)\right)\right]$$

$$P_{Q,\alpha} \triangleq (I - N_{Q,\alpha} S\, M_{Q,\alpha})^{-1} N_{Q,\alpha} \tag{A7}$$

$$T_Q \triangleq S\, M_{Q,\alpha} P_{Q,\alpha} + I_n \tag{A8}$$

Summary of Solution Procedure

Step 1: Compute S, $M_{Q,\alpha}$, and $N_{Q,\alpha}$ satisfying, respectively, Eqs. (A4–A6).
Step 2: Compute $P_{Q,\alpha}$ satisfying Eq. (A7).
Step 3: Compute T_Q satisfying Eq. (A8).
Step 4: Compute $\bar{Q}$ satisfying

$$\text{vec}\,(\bar{Q}) = T_Q S\, \text{vec}(\bar{V})$$

Step 5: Compute Q satisfying Eq. (A3) or equivalently

$$Q = \Psi \bar{Q} \Psi^H$$

Remark A.1. An intermediate step in the derivation of the solution procedure is that

$$\text{vec}\left(M(\bar{Q})\right) = M_{Q,\alpha} z(\bar{Q})$$

where

$$z(\bar{Q}) \triangleq \begin{bmatrix} z_{11}(\bar{Q}) \\ z_{22}(\bar{Q}) \\ z_{12}(\bar{Q}) \end{bmatrix}$$

and

$$z_{11,i}(\bar{Q}) \triangleq \alpha_i^2 \Psi(k+1), :)\bar{Q}\Psi^H(:, k+1)$$

$$z_{22,i}(\bar{Q}) \triangleq \alpha_i^2 \Psi(k, :)\bar{Q}\Psi^H(:, k)$$

$$z_{12,i}(\bar{Q}) \triangleq -\alpha_i^2 \Psi(k+1, :)\bar{Q}\Psi^H(k, :)$$

Appendix B: Efficient Computation of the Solution to Four Coupled Lyapunov Equations for Differentiation and Correction

This Appendix develops a solution procedure for efficiently solving for P, Q, $\hat{P}$, and $\hat{Q}$ satisfying the four $n \times n$ coupled Lyapunov equations

$$0 = A_P^T + PA_P + R + \sum_{i=1}^{n_\alpha} \alpha_i^2 A_i^T P A_i + \sum_{i=1}^{n_\alpha} \alpha_i^2 A_i^T \hat{P} A_i \tag{B1}$$

$$0 = A_Q Q + QA_Q^T + V + \sum_{i=1}^{n_\alpha} \alpha_i^2 A_i Q A_i^T + \sum_{i=1}^{n_\alpha} \alpha_i^2 A_i \hat{Q} A_i^T \tag{B2}$$

$$0 = A_Q^T \hat{P} + \hat{P} A_Q + \hat{R} + G_C Q \hat{F} + \hat{F} Q G_C + H_P^H P + P H_P \tag{B3}$$

$$0 = A_P \hat{Q} + \hat{Q} A_Q^T + \hat{V} + G_B P \hat{E} + \hat{E} P G_B + H_Q Q + Q H_Q^H \tag{B4}$$

where A_i is defined by Eq. (A2). It is assumed that Eqs. (B1–B4) have a unique solution $(P, Q, \hat{P}, \hat{Q})$. It is also assumed that A_P and A_Q are nondefective. The solution procedure is based on transforming A_P and A_Q to complex diagonal matrices. The results of Appendix A are used extensively. The actual solution procedure is summarized at the end of this Appendix.

Let Ψ_P and Ψ_Q be the eigenvector matrix of A_P and A_Q, such that

$$A_P = \Psi_P \Lambda_P \Psi_p^{-1}, \qquad A_Q = \Psi_Q \Lambda_Q \Psi_Q^{-1} \tag{B5}$$

where $\Lambda_P \in \mathbb{C}^{n \times n}$ and $\Lambda_Q \in \mathbb{C}^{n \times n}$ are diagonal. Substituting Eqs. (B5) into Eqs. (B1–B4) yields

$$0 = \Lambda_P^H \bar{P} + \bar{P}\Lambda_P + \bar{R} + M_P(\bar{P}) + \hat{M}_P(\bar{\hat{P}}) \tag{B6}$$

$$0 = \Lambda_Q \bar{Q} + \bar{Q}\Lambda_Q^H + \bar{V} + M_Q(\bar{Q}) + \hat{M}_Q(\bar{\hat{Q}}) \tag{B7}$$

$$0 = \Lambda_Q^H \bar{\hat{P}} + \bar{\hat{P}}\Lambda_Q + \bar{\hat{R}} + \bar{G}_C \bar{Q} \bar{\hat{F}} + \bar{\hat{F}} \bar{Q} \bar{G}_C + \bar{H}_P^H \bar{P} \bar{K}_P + \bar{K}_P^H \bar{P} \bar{H}_P \tag{B8}$$

$$0 = \Lambda_P \bar{\hat{Q}} + \bar{\hat{Q}}\Lambda_P^H + \bar{\hat{V}} + \bar{G}_B \bar{P} \bar{\hat{E}} + \bar{\hat{E}} \bar{P} \bar{G}_B + \bar{H}_Q \bar{Q} \bar{K}_Q^H + \bar{K}_Q \bar{Q} \bar{H}_Q^H \tag{B9}$$

where

$$\bar{P} = \Psi_P^H P \Psi_P, \qquad \bar{Q} = \Psi_Q^{-1} Q \Psi_Q^{-H} \tag{B10}$$

$$\bar{\hat{P}} = \Psi_Q^H \hat{P} \Psi_Q, \qquad \bar{\hat{Q}} = \Psi_P^{-1} \hat{Q} \Psi_P^{-H} \tag{B11}$$

$$\bar{R} = \Psi_P^H R \Psi_P, \qquad \bar{V} = \Psi_Q^{-1} V \Psi_Q^{-H}$$

$$\bar{\hat{R}} = \Psi_Q^H \hat{R} \Psi_Q, \qquad \bar{\hat{V}} = \Psi_P^{-1} \hat{V} \Psi_P^{-H}$$

$$M_P(\bar{P}) = \sum_{i=1}^{n_\alpha} \alpha_i^2 \Psi_P^H A_i^T \Psi_P^{-H} \bar{P} \Psi_P^{-1} A_i \Psi_P$$

$$\hat{M}_P(\bar{P}) = \sum_{i=1}^{n_\alpha} \alpha_i^2 \Psi_P^H A_i^T \Psi_Q^{-H} \bar{\hat{P}} \Psi_Q^{-1} A_i \Psi_P$$

$$M_Q(\bar{Q}) = \sum_{i=1}^{n_\alpha} \alpha_i^2 \Psi_Q^{-1} A_i \Psi_Q \bar{Q} \Psi_Q^H A_i^T \Psi_Q^{-H}$$

$$\hat{M}_Q(\bar{\hat{Q}}) = \sum_{i=1}^{n_\alpha} \alpha_i^2 \Psi_Q^{-1} A_i \Psi_P \bar{\hat{Q}} \Psi_P^H A_i^T \Psi_Q^{-H}$$

$$\bar{G}_C = \Psi_Q^H G_C \Psi_Q, \qquad \bar{G}_B = \Psi_P^{-1} G_B \Psi_P^{-H}$$

$$\bar{\hat{F}} = \Psi_Q^H \hat{F} \Psi_Q, \qquad \bar{\hat{E}} = \Psi_P^{-1} \hat{E} \Psi_P^{-H}$$

$$\bar{H}_P = \Psi_P^{-1} H_P \Psi_Q, \qquad \bar{H}_Q = \Psi_P^{-1} H_Q \Psi_Q$$

$$\bar{K}_P = \Psi_P^{-1} \Psi_Q, \qquad \bar{K}_Q = \Psi_P^{-1} \Psi_Q$$

For $\lambda \in \mathbb{R}^n$ and $\Psi \in \mathbb{R}^{n\times n}$ the functions **seig, malpha,** and **nalpha** are defined as follows:

$$S = \mathbf{seig}(\lambda)$$

is equivalent to

$$S = \left[-\operatorname{diag}(\lambda\omega_n^T + \omega_n\lambda^H)\right]^{-1}$$

$$M_\alpha = \mathbf{malpha}(\Psi)$$

is equivalent to

$$M_\alpha = \left[M_\alpha^{(1)}\ M_\alpha^{(2)}\ M_\alpha^{(3)}\right]$$

where

$$M_\alpha^{(1)} = \left(\omega_n \otimes \Psi(:,\ell_\alpha)\right) * \left(\Psi^*(:,\ell_\alpha)\otimes\omega_n\right)$$

$$M_\alpha^{(2)} = \left(\omega_n \otimes \Psi(:,\ell_\alpha+\omega_{n_\alpha})\right) * \left(\Psi(:,\ell_\alpha+\omega_{n_\alpha})\otimes\omega_n\right)$$

$$M_\alpha^{(3)} = \left(\omega_n \otimes \Psi(:,\ell_\alpha)\right) * \left(\Psi(:,\ell_\alpha+\omega_{n_\alpha})\otimes\omega_n\right) + \left(\omega_n \otimes \Psi(:,\ell_\alpha+\omega_{n_\alpha})\right) * \left(\Psi(:,\ell_\alpha)\otimes\omega_n\right)$$

$$N_\alpha = \mathbf{nalpha}(\Psi)$$

is equivalent to

$$N_\alpha = \begin{bmatrix} N_\alpha^{(1)} \\ N_\alpha^{(2)} \\ N_\alpha^{(3)} \end{bmatrix}$$

where

$$N_\alpha^{(1)} = \left((\alpha*\alpha)\omega_{n^2}^T\right) * \left[\left(\Psi^*(\ell_\alpha+\omega_{n_\alpha},:)\otimes\omega_n^T\right) + \left(\omega_n^T\otimes\Psi(\ell_\alpha+\omega_{n_\alpha},:)\right)\right]$$

$$N_\alpha^{(2)} = \left((\alpha*\alpha)\omega_{n^2}^T\right) * \left[\left(\Psi^*(\ell_\alpha,:)\otimes\omega_n^T\right) + \left(\omega_n^T\otimes\Psi(\ell_\alpha,:)\right)\right]$$

$$N_\alpha^{(3)} = -\left((\alpha*\alpha)\omega_{n^2}^T\right) * \left[\left(\Psi^*(\ell_\alpha+\omega_{n_\alpha},:)\otimes\omega_n^T\right) * \left(\omega_n^T\otimes\Psi(\ell_\alpha,:)\right)\right]$$

It follows from the results of Appendix A that Eqs. (B6) and (B7) can be expressed as

$$\operatorname{vec}(\bar{P}) = T_P S_P \operatorname{vec}\left(\hat{M}_P(\bar{\bar{P}})\right) + T_P S_P \operatorname{vec}(\bar{R}) \tag{B12}$$

$$\operatorname{vec}(\bar{Q}) = T_Q S_Q \operatorname{vec}\left(\hat{M}_Q(\bar{\bar{Q}})\right) + T_Q S_Q \operatorname{vec}(\bar{V}) \tag{B13}$$

where

$$T_P = (S_P M_{P,\alpha} P_{P,\alpha} + I_n), \qquad T_Q = (S_Q M_{Q,\alpha} Q_{Q,\alpha} + I_n)$$

$$P_{P,\alpha} = (I_n - N_{P,a} S_P M_{P,\alpha})^{-1} N_{P,\alpha}$$

$$Q_{Q,\alpha} = (I_n - N_{Q,a} S_Q M_{Q,\alpha})^{-1} N_{Q,\alpha}$$

$$S_P = \mathbf{seig}(\lambda_P^*), \qquad S_Q = \mathbf{seig}(\lambda_Q)$$

$$\lambda_P = [\Lambda_{P,11}\ \Lambda_{P,22}\ \cdots\ \Lambda_{P,nn}]^T$$

$$\lambda_Q = [\Lambda_{Q,11}\ \Lambda_{Q,22}\ \cdots\ \Lambda_{Q,nn}]^T$$

$$M_{P,\alpha} = \mathbf{malpha}(\Psi_P^*), \qquad M_{Q,\alpha} = \mathbf{malpha}(\Psi_Q^{-1})$$

$$N_{P,\alpha} = \mathbf{nalpha}(\Psi_P^{-*}), \qquad N_{Q,\alpha} = \mathbf{nalpha}(\Psi_Q)$$

Using standard Kronecker algebra, we can express Eqs. (B8) and (B9) as

$$\operatorname{vec}(\bar{\bar{P}}) = S_Q^* U_{P,1}\operatorname{vec}(\bar{P}) + S_Q^* U_{Q,1}\operatorname{vec}(\bar{Q}) + S_Q^*\operatorname{vec}(\bar{\bar{R}}) \tag{B14}$$

$$\operatorname{vec}(\bar{\bar{Q}}) = S_P^* U_{P,2}\operatorname{vec}(\bar{P}) + S_P^* U_{Q,2}\operatorname{vec}(\bar{Q}) + S_P^*\operatorname{vec}(\bar{\bar{V}}) \tag{B15}$$

where

$$\begin{aligned} U_{P,1} &= \left(\bar{K}_P^T\otimes\bar{H}_P^H\right) + \left(\bar{H}_P^T\otimes\bar{K}_P^H\right) \\ U_{Q,1} &= \left(\bar{F}^T\otimes\bar{G}_C\right) + \left(\bar{G}_C^T\otimes\bar{F}\right) \end{aligned} \tag{B16}$$

$$\begin{aligned} U_{P,2} &= \left(\bar{\bar{E}}^T\otimes\bar{G}_B\right) + \left(\bar{G}_B^T\otimes\bar{\bar{E}}\right) \\ U_{Q,2} &= (\bar{K}_Q^*\otimes\bar{H}_Q) + (\bar{H}_Q^*\otimes\bar{K}_Q) \end{aligned} \tag{B17}$$

Now, from the results of Appendix A, we can write

$$\operatorname{vec}\left(\hat{M}_P(\bar{\bar{P}})\right) = M_{P,\alpha} z(\bar{\bar{P}}), \qquad \operatorname{vec}\left(\hat{M}_Q(\bar{\bar{Q}})\right) = M_{Q,\alpha} z(\bar{\bar{Q}}) \tag{B18}$$

$$z(\bar{\bar{P}}) = \hat{N}_{P,\alpha}\operatorname{vec}(\bar{\bar{P}}), \qquad z(\bar{\bar{Q}}) = \hat{N}_{Q,\alpha}\operatorname{vec}(\bar{\bar{Q}}) \tag{B19}$$

where

$$\hat{N}_{P,\alpha} = \mathbf{nalpha}(\Psi_Q^{-*}), \qquad \hat{N}_{Q,\alpha} = \mathbf{nalpha}(\Psi_P)$$

Substituting, Eqs. (B12) and (B13) into Eqs. (B14) and (B15) gives

$$\begin{aligned} \operatorname{vec}(\bar{\bar{P}}) &= S_Q^* U_{P,1} T_P S_P \operatorname{vec}\left(\hat{M}_P(\bar{\bar{P}})\right) \\ &\quad + S_Q^* U_{Q,1} T_Q S_Q \operatorname{vec}\left(\hat{M}_Q(\bar{\bar{Q}})\right) + \hat{p}_0 \end{aligned} \tag{B20}$$

$$\begin{aligned} \operatorname{vec}(\bar{\bar{Q}}) &= S_P^* U_{P,2} T_P S_P \operatorname{vec}\left(\hat{M}_P(\bar{\bar{P}})\right) \\ &\quad + S_P^* U_{Q,2} T_Q S_Q \left(\hat{M}_Q(\bar{\bar{Q}})\right) + \hat{q}_0 \end{aligned} \tag{B21}$$

where

$$\hat{p}_0 = S_Q^* U_{P,1} T_P S_P \operatorname{vec}(\bar{R}) + S_Q^* U_{Q,1} T_Q S_Q \operatorname{vec}(\bar{V}) + S_Q^* \operatorname{vec}(\bar{\bar{R}}) \tag{B22}$$

$$\hat{q}_0 = S_P^* U_{P,2} T_P S_P \operatorname{vec}(\bar{R}) + S_P^* U_{Q,2} T_Q S_Q \operatorname{vec}(\bar{V}) + S_P^* \operatorname{vec}(\bar{\bar{V}}) \tag{B23}$$

Substituting Eqs. (B18) into Eqs. (B20) and (B21) gives

$$\begin{aligned} \operatorname{vec}(\bar{\bar{P}}) &= S_Q^* U_{P,1} T_P S_P M_{P,\alpha} z(\bar{\bar{P}}) \\ &\quad + S_Q^* U_{Q,1} T_Q S_Q M_{Q,\alpha} z(\bar{\bar{Q}}) + \hat{p}_0 \end{aligned} \tag{B24}$$

$$\begin{aligned} \operatorname{vec}(\bar{\bar{Q}}) &= S_P^* U_{P,2} T_P S_P M_{P,\alpha} z(\bar{\bar{P}}) \\ &\quad + S_P^* U_{Q,2} T_Q S_Q M_{Q,\alpha} z(\bar{\bar{Q}}) + \hat{q}_0 \end{aligned} \tag{B25}$$

Substituting Eqs. (B24) and (B25) into Eq. (B19) gives

$$\begin{aligned} z(\bar{\bar{P}}) &= \hat{N}_{P,\alpha} S_Q^* U_{P,1} T_P S_P M_{P,\alpha} z(\bar{\bar{P}}) \\ &\quad + \hat{N}_{P,\alpha} S_Q^* U_{Q,1} T_Q S_Q M_{Q,\alpha} z(\bar{\bar{Q}}) + \hat{N}_{P,\alpha}\hat{p}_0 \\ z(\bar{\bar{Q}}) &= \hat{N}_{Q,\alpha} S_P^* U_{P,2} T_P S_P M_{P,\alpha} z(\bar{\bar{P}}) \\ &\quad + \hat{N}_{Q,\alpha} S_P^* U_{Q,2} T_Q S_Q M_{Q,\alpha} z(\bar{\bar{Q}}) + \hat{N}_{Q,\alpha}\hat{q}_0 \end{aligned}$$

or, equivalently,

$$\begin{bmatrix} D_{11} & D_{12} \\ D_{21} & D_{22} \end{bmatrix} \begin{bmatrix} z(\bar{P}) \\ z(\bar{Q}) \end{bmatrix} = \begin{bmatrix} \hat{N}_{P,\alpha}\hat{p}_0 \\ \hat{N}_{Q,\alpha}\hat{q}_0 \end{bmatrix} \tag{B26}$$

where

$$D_{11} = I_{3n_\alpha} - \hat{N}_{P,\alpha} S_Q^* U_{P,1} T_P S_P M_{P,\alpha}$$
$$D_{12} = -\hat{N}_{P,\alpha} S_Q^* U_{Q,1} T_Q S_Q M_{Q,\alpha} \tag{B27}$$

$$D_{21} = -\hat{N}_{Q,\alpha} S_P^* U_{P,2} T_P S_P M_{P,\alpha}$$
$$D_{22} = I_{3n_\alpha} - \hat{N}_{Q,\alpha} S_P^* U_{Q,2} T_Q S_Q M_{Q,\alpha} \tag{B28}$$

Finally, substituting Eqs. (B18) into Eqs. (B12) and (B13) gives

$$\mathrm{vec}(\bar{P}) = T_P S_P M_{P,\alpha} z(\bar{P}) + T_P S_P \mathrm{vec}(\bar{R}) \tag{B29}$$

$$\mathrm{vec}(\bar{Q}) = T_Q S_Q M_{Q,\alpha} z(\bar{Q}) + T_Q S_Q \mathrm{vec}(\bar{V}) \tag{B30}$$

Notice from Eqs. (B16) and (B17) that $U_{P,1}$, $U_{Q,1}$, $U_{P,2}$, and $U_{Q,2}$ are each an $n^2 \times n^2$ matrix. The storage required to compute these matrices is hence very large for large n. To avoid this memory requirement it is possible to compute $\hat{p}_0$ and $\hat{q}_0$ satisfying Eqs. (B22) and (B23) and D_{11}, D_{12}, D_{21}, and D_{22} satisfying Eqs. (B27) using the identity

$$\mathrm{vec}(ADB) = (B^T \otimes A)\mathrm{vec}(D)$$

By substituting Eqs. (B16) and (B17) into Eqs. (B19), (B27), and (B28), and using Eq. (B29), it follows that $\hat{p}_0$, $\hat{q}_0$, D_{11}, D_{12}, D_{21}, and D_{22} can be computed using the following algorithms. In these algorithms $\mathrm{vec}_n^{-1} : \mathbb{R}^n \to \mathbb{R}^{n \times n}$ is understood to be the operator satisfying

$$M = \mathrm{vec}_n^{-1}\big(\mathrm{vec}(M)\big)$$

Algorithm for computation of $\hat{p}_0$ and $\hat{q}_0$:

$$W_P = \mathrm{vec}_n^{-1}\big((M_{P,\alpha} P_{P,\alpha} + I_n) S_P \mathrm{vec}(R)\big)$$
$$W_Q = \mathrm{vec}_n^{-1}\big((M_{Q,\alpha} P_{Q,\alpha} + I_n) S_Q \mathrm{vec}(V)\big)$$
$$\hat{p}_0 = \mathrm{vec}\big((G_c W_Q \hat{F} + H_P^H W_P K_P) + (G_c W_Q \hat{F} + H_P^H W_P K_P)^H + \hat{R}\big)$$
$$\hat{q}_0 = \mathrm{vec}\big((G_B W_P \hat{E} + H_Q W_Q K_Q^H) + (G_B W_P \hat{E} + H_Q W_Q K_Q^H)^H + \hat{V}\big)$$

Algorithm for computation of D_{11}, D_{12}, D_{21}, and D_{22}:

$$V_P = T_P S_P M_{P,\alpha}, \qquad V_Q = T_Q S_Q M_{Q,\alpha}$$

for $i = 1 : 3n_\alpha$

$$D_{11}(:, i) = I_{3n_\alpha} - \hat{N}_{P,\alpha} S_Q^* \mathrm{vec}\big(H_P^H V_P(:, i) K_P + K_P^H V_P(:, i)^H H_P\big)$$
$$D_{12}(:, i) = -\hat{N}_{P,\alpha} S_Q^* \mathrm{vec}\big(G_c V_Q(:, i)\hat{F} + \hat{F}^H V_Q(:, i)^H G_c^H\big)$$
$$D_{21}(:, i) = -\hat{N}_{Q,\alpha} S_P^* \mathrm{vec}\big(H_Q V_P(:, i)\hat{K}_Q^H + K_Q V_P(:, i)^H H_Q^H\big)$$
$$D_{22}(:, i) = I_{3n_\alpha} - \hat{N}_{Q,\alpha} S_P^* \big(H_Q V_Q(:, i) K_Q^H + K_Q V_Q(:, i)^H H_Q^H\big)$$

Summary of Solution Procedure

Step 1: Construct D_{11}, D_{12}, D_{21}, and D_{22} and solve Eq. (B26) for $z(\bar{P})$ and $z(\bar{Q})$.

Step 2: Solve Eqs. (B29) and (B30) for $\bar{P}$ and $\bar{Q}$.

Step 3: Solve Eqs. (B24) and (B25) for $\hat{\bar{P}}$ and $\hat{\bar{Q}}$.

Step 4: Compute P, Q, $\hat{P}$, and $\hat{Q}$, satisfying Eqs. (B10) and (B11), or equivalently

$$P = \Psi_P^{-H} \bar{P} \Psi_P^{-1}, \qquad Q = \Psi_Q \bar{Q} \Psi_Q^H$$
$$\hat{Q} = \Psi_Q^{-H} \hat{\bar{P}} \Psi_Q^{-1}, \qquad \hat{Q} = \Psi_P \hat{\bar{Q}} \Psi_P^H$$

Acknowledgments

This work was supported by Sandia National Laboratories under Contract 54-7609 and the Air Force Office of Scientific Research under Contract F49620-91-0019.

References

[1]Kwakernaak, H., and Sivan, R., *Linear Optimal Control Systems*, Wiley, New York, 1972.

[2]Doyle, J. C., "Guaranteed Margins for LQG Regulators," *IEEE Transactions on Automatic Control*, Vol. 23, Aug. 1978, pp. 756, 757.

[3]Hyland, D. C., "Maximum Entropy Stochastic Approach to Controller Design for Uncertain Structural Systems," *Proceedings of the American Control Conference* (Arlington, VA), IEEE, Piscataway, NJ, 1982, pp. 680–688.

[4]Bernstein, D. S., and Hyland, D. C., "The Optimal Projection/Maximum Entropy Approach to Designing Low-Order, Robust Controllers for Flexible Structures," *Proceedings of the IEEE Conference on Decision and Control* (Fort Lauderdale, FL), IEEE, Piscataway, NJ, 1985, pp. 745–752.

[5]Bernstein, D. S., and Hyland, D. C., "The Optimal Projection Approach to Robust, Fixed-Structure Control Design," *Mechanics and Control of Large Flexible Structures*, edited by J. L. Junkins, AIAA, Washington, DC, 1990, pp. 237–293.

[6]Collins, E. G., Jr., Phillips, D. J., and Hyland, D. C., "Robust Decentralized Control Laws for the ACES Structure," *Control Systems Magazine*, Vol. 11, April 1991, pp. 62–70.

[7]Collins, E. G., Jr., King, J. A., Phillips, D. J., and Hyland, D. C., "High Performance, Accelerometer-Based Control of the Mini-MAST Structure," *Journal of Guidance, Control, and Dynamics*, Vol. 15, No. 4, 1992, pp. 885–892.

[8]Davis, L. D., Hyland, D. C., and Bernstein, D. S., "Application of the Maximum Entropy Design Approach to the Space Control Laboratory Experiment (SCOLE)," Final Rept. for NASA Contract NAS1-17741, NASA Langley Research Center, Langley, VA, Jan. 1985.

[9]Cheung, M.-F., and Yurkovich, S., "On the Robustness of MEOP Design Versus Asymptotic LQG Synthesis," *IEEE Transactions on Automatic Control*, Vol. 33, Nov. 1988, pp. 1061–1065.

[10]Collins, E. G., Jr., King, J. A., and Bernstein, D. S., "Application of Maximum Entropy/Optimal Projection Design Synthesis to a Benchmark Problem," *Journal of Guidance, Control, and Dynamics*, Vol. 15, No. 5, 1992, pp. 1094–1102.

[11]Bernstein, D. S., Haddad, W. M., Hyland, D. C., and Tyan, F., "A Maximum Entropy-Type Lyapunov Function for Robust Stability and Performance Analysis," *Systems and Control Letters*, Vol. 12, 1993, pp. 73–87.

[12]Haddad, W. M., and Bernstein, D. S., "Parameter-Dependent Lyapunov Functions, Constant Real Parameter Uncertainty, and the Popov Criterion in Robust Analysis and Synthesis: Part 1, Part 2," *Proceedings of the IEEE Conference on Decision and Control* (Brighton, England, UK), IEEE, Piscataway, NJ, 1991, pp. 2274–2279, 2617–2623.

[13]Collins, E. G., and Richter, S., "A Homotopy Algorithm for Synthesizing Robust Controllers for Flexible Structures Via the Maximum Entropy Design Equations," *Third Air Force/NASA Symposium on Recent Advances in Multidisciplinary Analysis and Optimization* (San Diego, CA), May 1990, pp. 1449–1454.

[14]Brewer, J. W., "Kronecker Products and Matrix Calculus in System Theory," *IEEE Transactions on Circuit and Systems*, Vol. CAS-25, No. 9, 1978, pp. 772–781.

[15]Garcia, C. B., and Zangwill, W. I., *Pathways to Solutions, Fixed Points and Equilibria*, Prentice-Hall, Englewood Cliffs, NJ, 1981.

[16]Richter, S. L., and DeCarlo, R. A., "Continuation Methods: Theory and Applications," *IEEE Transactions on Circuits and Systems*, Vol. CAS-30, No. 6, 1983, pp. 347–352.

[17]Watson, L. T., "ALGORITHM 652 HOMPACK: A Suite of Codes for Globally Convergent Homotopy Algorithms," *ACM Transactions on Mathematical Software*, Vol. 13, Sept. 1987, pp. 281–310.

[18]Fletcher, R., *Practical Methods of Optimization*, Wiley, New York, 1987.

[19]Richter, S., Davis, L. D., and Collins, E. G., Jr., "Efficient

Computation of the Solutions to Modified Lyapunov Equations," *SIAM Journal of Matrix Analysis and Applications*, Vol. 14, No. 2, 1993, pp. 420–434.

[20]Collins, E. G., Jr., Davis, L. D., and Richter, S., "Homotopy Algorithms for H_2 Optimal Reduced-Order Dynamic Compensation and Maximum Entropy Control," Final Rept. for Contract 54-7609, Sandia National Lab., Albuquerque, NM, Aug. 1992.

[21]Irwin, R. D., Jones, V. L., Rice, S. A., Seltzer, S. M., and Tollison, D. J., "Active Control Technique Evaluation for Spacecraft (ACES)," Final Rept. to Flight Dynamics Lab. of Wright Aeronautical Labs, AFWAL-TR-88-3038, Wright-Patterson AFB, OH, June 1988.

[22]Collins, E. G., Jr., Haddad, W. M., and Davis, L. D., "Riccati Equation Approaches for Small Gain, Positivity, and Popov Robustness Analysis," *Journal of Guidance, Control, and Dynamics*, Vol. 17, No. 2, 1994, pp. 322–329; also *Proceedings of the 1993 American Control Conference*, IEEE, Piscataway, NJ, 1993, pp. 1079–1083.

[23]Yousuff, A., and Skelton, R. E., "A Note on Balanced Controller Reduction," *IEEE Transactions on Automatic Control,* Vol. AC-29, March 1984, pp. 254–257.